Talanta 200 (2019) 57–66

Contents lists available at ScienceDirect

Talanta

journal homepage: www.elsevier.com/locate/talanta

A chemiluminescence biosensor for lysozyme detection based on aptamers and hemin/G-quadruplex DNAzyme modified sandwich-rod carbon fiber composite

Yuanling Sun, Yanna Lin, Rui Han, Xueying Wang*, Chuannan Luo*

Key Laboratory of Interfacial Reaction & Sensing Analysis in Universities of Shandong, School of Chemistry and Chemical Engineering, University of Jinan, Jinan 250022, PR China

ARTICLE INFO

Keywords:
Aptamers
Carbon fiber
Graphene
Lysozyme
Chemiluminescence biosensor

ABSTRACT

In our work, aptamers and hemin/G-quadruplex DNAzyme modified sandwich-rod graphene quantum dots @ graphene oxide @ carbon fiber composite (DNAzyme/L-Apt/GQDs@GO@CF) was successfully prepared for sensitive and selective chemiluminescence (CL) detection of lysozyme (LZM). Initially, GQDs@GO@CF was successfully prepared and characterized. Lysozyme aptamers (L-Apt) as a recognition element and hemin/G-quadruplex DNAzyme (DNAzyme) as a catalyst of luminal - H_2O_2 were modified on the surface of GQDs@GO@CF, sequentially. The immobilization properties of GQDs@GO@CF to L-Apt and the adsorption properties of L-Apt/GQDs@GO@CF to DNAzyme were also researched, respectively. Then, the modified sandwich-rod carbon fiber composite was applied to the construction of CL biosensor for LZM detection. When LZM existed, DNAzyme would be released from the surface of L-Apt/GQDs@GO@CF and catalyzed the reaction of luminal - H_2O_2. Under optimized conditions, the CL biosensor for LZM detection showed wide linear range of 2.64×10^{-10} to 6.6×10^{-8} g/L and low detection limit of 1.25×10^{-11} g/L (3δ). Finally, the CL biosensor was successfully used for LZM detection in human urine samples and illustrated the potential application in pratical samples.

1. Introduction

Lysozyme (LZM), also known as muramidase or N-acetylmuramide, is an alkaline enzyme in pathogenic bacteria [1,2]. Owing to its excellent bactericidal properties, lytic activation and low molecular weight, LZM has been widely applied in food industry as preservative or biomedical sciences as therapeutic agent [3–5]. LZM in serum is a marker for various kinds of acute leukemia [6], and LZM in urine is also significant for the evaluation of renal tubular damage, high lysozyme hyperlipidemia, renal damage and other diseases [7]. Therefore, sensitive and accurate detection of LZM is extremely important [8]. There are already some methods for LZM detection, such as resonance rayleigh-scattering [9], electrochemical biosensor [10,11], fluorescence biosensor [12], chemiluminescence (CL) method based molecularly imprinted polymers (MIPs) [13], aptamer-based biosensor [14]. These methods could meet certain requirements in some fields, but some were trapped in its complex operation, expensive instruments, low selectivity or sensitivity [15]. So finding a simple, cost-effective, sensitive and selective method to detect LZM is urgent needed.

Chemiluminescence (CL) is an optical radiation phenomenon accompanying in process of chemical reaction [16]. The product molecules can absorb energy from chemical reactions and jumped to an excited state, then the excited state molecules generate light radiation when returning to the ground state. Because of its high sensitivity, convenient operation, wide detection range and easy to automate, CL has attracted researchers' attention in recent years. However, low selectivity limits its applications in some areas, which could be improved by some specific identification materials, such as molecularly imprinted polymers (MIPs) [17], antigen-antibody materials [18] and aptamers composites [19,20]. Besides, CL intensity (*I*) of chemical reactions are usually weak and catalysts are needed [21]. Common catalysts in CL reactions are metal nanoparticles [22], carbon nanoparticles [23] and enzymes (including some simulated enzymes) [24,25].

Aptamers are some specific oligonucleotide sequence screened from artificial single-stranded oligonucleotide libraries [26]. Compared with antibodies, aptamers have high specificity and affinity to their multiple classes of target molecules, such as proteins, amino acids, drugs and inorganic ions. Moreover, aptamers show many advantages of good

* Corresponding authors.
E-mail addresses: chm_wangxy@ujn.edu.cn (X. Wang), chm_yfl518@163.com (C. Luo).

https://doi.org/10.1016/j.talanta.2019.03.007
Received 10 December 2018; Received in revised form 19 February 2019; Accepted 2 March 2019
Available online 02 March 2019
0039-9140/

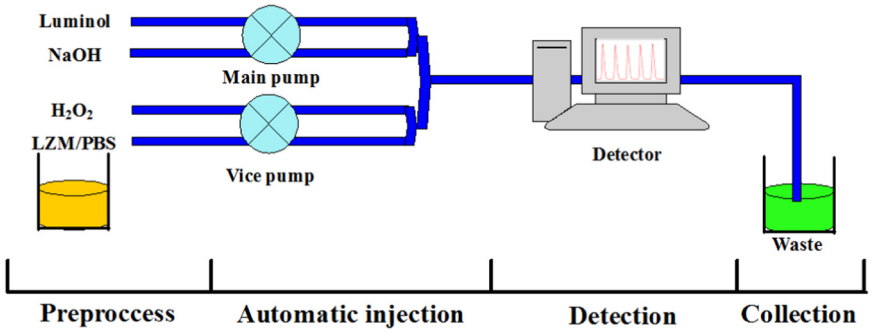

Fig. 1. The schematic of IFFM-E flow injection CL analyzer.

stability, easy to obtain, simple synthesis, easy to modify or label [27]. So aptamers have been widely used in biosensors construction [28]. Si et al. [29] prepared a biosensor to detect cancer biomarker CEA based on aptamer induced current and molybdophosphate captured on a glassy carbon electrode. Zhang et al. [30] synthesized carbon-based nanocomposites with aptamer-templated silver nanoclusters and realized the highly sensitive and selective detection of platelet-derived growth factor (PDGF).

Carbon fiber (CF) is a kind of fiber materials with high strength and modulus. CF also has high quality density, soft outside and hard inside [31,32]. So CF is usually used as functional composites after appropriate modification and it has been used in the synthesis of smart materials, energy device devices and the construction of biosensors [33–36]. For its applications in biosensors, Shi et al. [37] proposed a novel, sensitive and convenient method to detect lappaconitine based on an electrostatic spinning carbon nanotube fiber modified glassy carbon electrode (GCE/ESCNF). The sensitive detection of dopamine was realized by PEDOT/graphene oxide coating on vivo carbon fiber electrodes by Taylor et al. [38].

Graphene (GR) was successfully separated from graphite with micro-mechanical stripping by British scientists in 2004 [39]. As a new two-dimensional atomic crystal, GR is composed by sp^2 hybrid carbon atoms and shows some excellent performances of mechanical, electrical and thermal, low cost and easy chemical modification [40]. Graphene oxide (GO) is a kind of oxidation product of GR [41]. The growing oxygen-containing functional groups make GO more active than GR. Based on the excellent properties of large surface area, good biocompatibility, rich functional groups and easy to surface modification [42], GO and its composites have caused widespread concern among researchers in many fields, such as electronic devices [43], biosensing [44] and adsorption or energy storage materials [45]. Graphene quantum dots (GQDs) are a new nano-carbon material in recent years and have many good performances of water solubility, stability, bright fluorescence characteristics and low toxicity [46,47]. In addition, GQDs can react with some chemical groups and functional molecules by covalent bond [48]. A common method to covalent modification is the acylation or esterification reaction between biological molecules and chemical groups. In addition, its surface modification can also be achieved by π-π interaction, ionic bond or hydrogen bond effect.

In this work, GQDs@GO@CF was successfully synthesized and characterized. Then, L-Apt was immobilized on the surface of GQDs@GO@CF to improve the composites' specific recognition ability. Subsequently, the simulated catalytic enzyme - DNAzyme was combined together with L-Apt by the base complementary pairing effect. The composite was used for the construction of CL biosensor to detect LZM. When LZM existed, DNAzyme would be released from the surface of L-Apt/GQDs@GO@CF owing to the strong specific recognition ability between LZM and L-Apt and released DNAzyme catalyzed CL reaction. So the highly selective and sensitive detection of LZM was achieved.

2. Experimental

2.1. Materials

CF (24 K) was provided by Hui Ping Carbon Fiber Weaving Co. Ltd. of Yixing (Jiangsu, China). Graphite powder was supplied by Hongyan Chemical Reagent Factory (Tianjin, China). Citric acid was purchased by Tianjin Damao Chemical Reagent Factory (Tianjin, China). Lysozyme (LZM), Bovine serum albumin (BSA), Bovine hemoglobin (Hb), glycine (Gly), Alanine aminotransferase (ALT), L-cysteine (Cys), ammonium carbonate (AC) and lactic acid (LA) were purchased from Solebo Biological Technology Co. Ltd. (Beijing, China). Sodium hydroxide, potassium permanganate, ethanol, hydrogen peroxide and all other common chemicals unless specified were analytical reagent grade and used without further purification. LZM aptamer: 5'- ATCAGGGCT AAAGAGTGCAGAGTTACTTAG-3' (10 OD) and the single stranded DNA sequence of G-quadruplex DNAzyme (ssDNA): 5'-TAGTCCCGACGTAT CGTATGTTCGTTGGGTAGGGCGGGTTGGG-3' (10 OD) were purchased from Sangon Biotech Company (Shanghai, China). Redistilled water was used throughout the work. Phosphate buffer (PBS, pH = 7.4, 0.01 mol/L) solution was used to prepare all LZM solutions in all experiments.

2.2. Apparatus

The IFFM-E flow injection CL analyzer (Xi'an Remex Electronic instrument High-Tech Ltd, China) was equipped with an automatic injection system and a detection system. In the flow injection system, luminol and NaOH flowed through the two channels of main pump into the mixing reaction system while H_2O_2 and samples (or PBS) flowed through the two channels of the vice pump, as shown in Fig. 1. The process of electrochemical deposition was performed on a CHI 660D electrochemistry workstation (Beijing Huake Putian Technology Co., Ltd. China), in which the classical three-electrode system was adopted and the working electrode was CF composites. Synthetic materials were characterized by Scanning Electron Microscopy (SEM, GUANTA FEG 250, FEI, America), Transmission Electron Microscopy (TEM, JEOL1400 microscope, Japan), X-ray Diffraction (XRD, Brooke AXS, Germany), Fluorescence Spectrophotometer (FL, Shimadzu RF-5301, Japan), UV–visible Spectrophotometer (UVUV–visPerkinAElmer, America), Fourie Transform Infrared Spectroscopy (FT-IR, PerkinElmer Corporation, America) and Brunauer-Emmett-Teller surface area measurement (BET, Quantachrome, America).

2.3. Preparation of GO

GO was prepared by a modified Hummers method [49]. Briefly, 1.0 g of graphite powder and 200 mL of mixed acid (V_{H2SO4}:V_{HNO3} = 8:1) were added into a three mouth flask. Then 6.0 g of potassium permanganate was added and stirred for 12 h at 90 °C. After that, 30% H_2O_2 was dropped. Finally, the mixture was centrifuged and washed by

0.2 mol/L HCl and water, respectively. GO was obtained after vacuum dried.

2.4. Preparation of GQDs

2 g of citric acid was added to a 25 mL of three beaker and heated for 20 min at 200 °C until the solution turned orange. Then 10 mg/mL of NaOH was dropped to obtain the light green transparent solution. The solution was adjusted to pH = 7 by 10 mg/mL of HCl.

2.5. Preparation of GQDs@GO@CF

Many 2 cm long of CF were washed with acetone, ethanol and water, respectively and then dried. Then the electrochemical workstation was supplied with 1.2 V constant voltage and electrodeposited for 100 s to obtain GQDs@GO@CF. In the three-electrode electrochemical workstation, CF was used as the working electrode, platinum wire as the counter electrode, Ag/AgCl as the reference electrode and 3 mg/mL of GO dispersions as electrolyte. Under similar experimental conditions, GO@CF was used as the working electrode and 5 mg/mL of GQDs dispersions electrode. The three electrodes were deposited for 100 s at a voltage of 1.2 V provided by the electrochemical workstation and the final composites - GQDs@GO@CF was obtained. The preparing process of GQDs@GO@CF was shown in Fig. 2.

2.6. Preparation of hemin/G-quadruplex DNAzyme (DNAzyme)

DNAzyme was prepared by ssDNA and hemin. 0.2 mL 1.5×10^{-2} g/L of hemin and 0.4 mL 2.0×10^{-2} g/L of ssDNA were mixed and incubated for 60 min at 37 °C. Then the incubated solution was centrifuged for 90 min at 9000 rpm and excess ssDNA was removed. After transferred to a 250 mL volumetric flask, the final 2.8×10^{-5} g/L of DNAzyme was prepared successfully, as shown in Fig. 2.

2.7. Immobilization experiments

2.7.1. Immobilization isotherm

Multiple parallel 0.1 g GQDs@GO@CF were placed into 50.0 mL colorimetric tubes, respectively. Then, different volume doses 2.0×10^{-5} g/L of L-Apt were added to these tubes, respectively. After that, these tubes were shaken for 1 h at 25 °C, respectively. After removal separation, the supernatants in these tubes were determined by the CL analyzer and immobilization capacities were calculated.

2.7.2. Immobilization dynamics

Multiple parallel 0.1 g GQDs@GO@CF were dispersed in 50.0 mL 1.0×10^{-6} g/L of L-Apt which then were shaken for 0.5, 1, 3, 5, 10, 15, 20, 25, 30 min, respectively. After removal separation, the supernatants in these tubes were determined by the CL analyzer and immobilization capacities were calculated.

2.7.3. Calculation formula of immobilization capacity

The immobilization capacity was calculated from the following formula:

$$Q_e = (c_0 - c_e)V/m$$

where Q_e (g/g) was the mass of L-Apt immobilized per unit mass of GQDs@GO@CF; c_0 (g/L) and c_e (g/L) were the concentrations of initial and balance L-Apt, respectively; V (L) was the total volume of the immobilization mixture and m (g) was the addition of GQDs@GO@CF.

2.8. Adsorption experiments

2.8.1. Adsorption isotherm

Multiple parallel 0.1 g of L-Apt/GQDs@GO@CF were placed into 50.0 mL colorimetric tubes, respectively. Then, different volume doses 2.8×10^{-5} g/L of DNAzyme were added to these tubes, respectively. After that, these tubes were shaken for 1 h at 25 °C, respectively. After removal separation, the supernatants in these tubes were determined by the CL analyzer and the adsorption capacities were calculated.

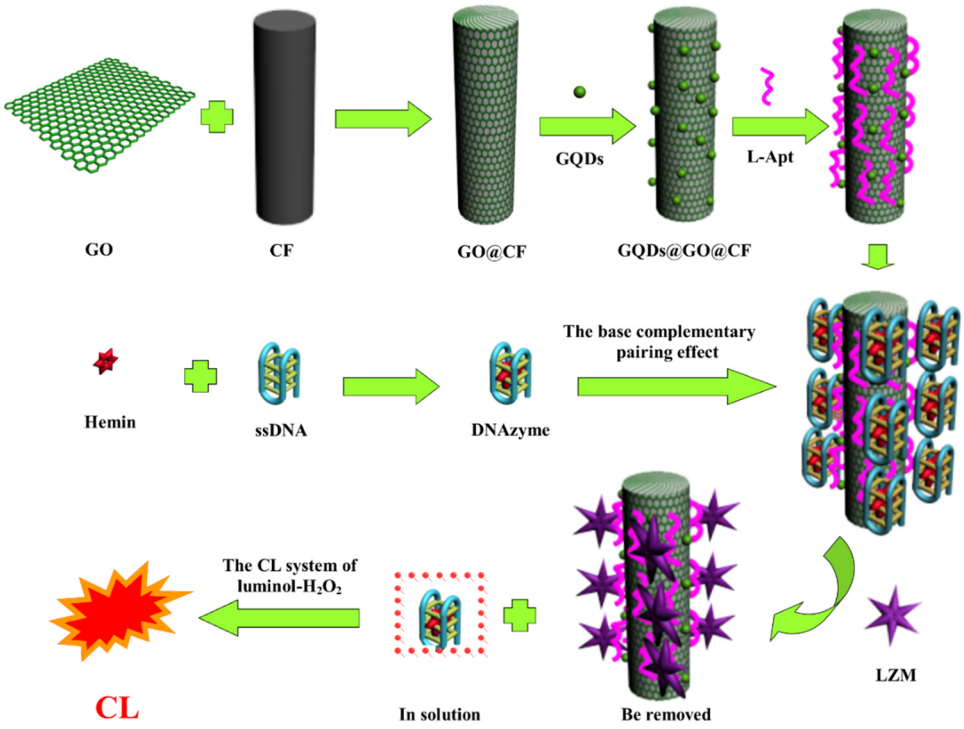

Fig. 2. The preparation process of composite and mechanism illustration of the CL biosensor.

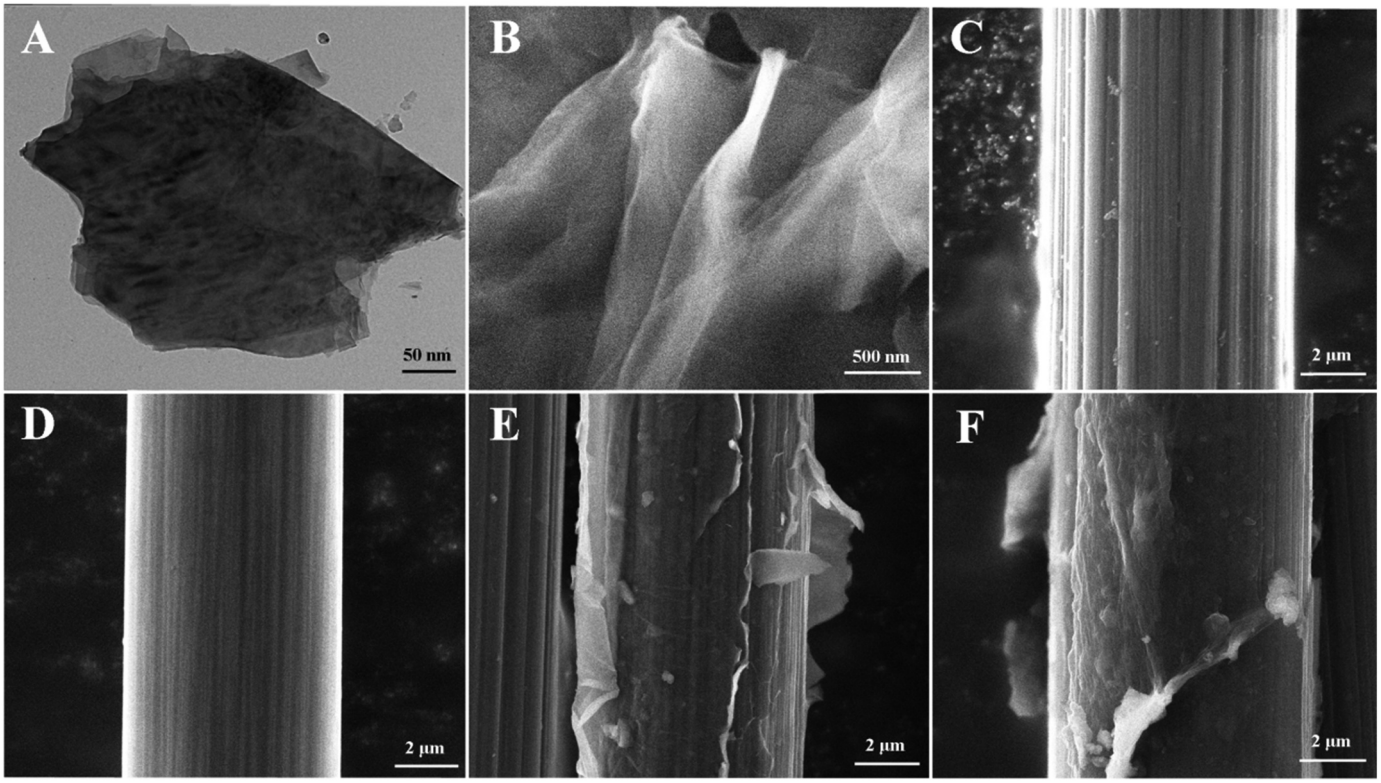

Fig. 3. The TEM image of GQDs (A); SEM images of GO (B), CF without pretreatment (C), CF with pretreatment (D), GO@CF (E) and GQDs@GO@CF (F).

2.8.2. Rebinding dynamics

Multiple parallel 0.1 g of L-Apt/GQDs@GO@CF were placed in 6.0 mL 8.0×10^{-7} g/L of DNAzyme which then were shaken for 0.5, 1, 3, 5, 10, 15, 20, 30 min, respectively. After removal separation, the supernatants in these tubes were determined by the CL analyzer and adsorption capacities were calculated.

2.8.3. Calculation formula of adsorption capacity

The adsorption capacity was calculated from the following formula:

$$Q'_e = (C'_0 - C'_e)V'/m'$$

where Q'_e (g/g) was the mass of DNAzyme adsorbed per unit mass of L-Apt/GQDs@GO@CF; c'_0 (g/L) and c'_e (g/L) were the concentrations of initial and balance DNAzyme, respectively; V' (L) was the total volume of adsorption mixture and m' (g) was the addition of L-Apt/GQDs@GO@CF.

2.9. Optimization experiments

To obtain the optimal CL intensity, pumps speed of the CL analyzer, concentrations of luminol, H_2O_2 and NaOH were all optimized by changing the single variable. For example, when the main pump speed was optimized, main pump speed varied during 20–45 r/min while other factors were fixed: 20 r/min of vice pump speed, 2.5×10^{-4} mol/L of luminol, 0.10 mol/L of H_2O_2 and 0.10 mol/L of NaOH.

2.10. Selectivity experiments

To study the selectivity of the proposed CL biosensor, selectivity experiments were carried out. In experiments, different amounts of interference substances were added to LZM standard solution (c_{LZM}: 8.0×10^{-8} g/L) to research their effects on the CL intensity. These effects were reflected by the interference multiples that is a concentration value relative to the concentration of LZM. Interference substances used in experiments were simulate urine components, such as bovine albumin (BSA), bovine hemoglobin (Hb), alanine aminotransferase (ALT), glycine (Gly), L-cysteine (Cys), ammonium carbonate (AC), lactic acid (LA), potassium ion (K^+) and chloride ion (Cl^-).

2.11. Recyclability experiments

To investigate practicality of the proposed CL biosensor, the recyclability of GQDs@GO@CF was researched by comparing the immobilization capacities of the GQDs@GO@CF used different times and unused before, respectively. In experiments, L-Apt was immobilized on the surface of GQDs@GO@CF by the π-π stacking effect between GQDs@GO@CF and L-Apt and different concentrations of LZM could cause the different changes of CL intensity.

2.12. Samples detection

LZM samples were detected by the CL analyzer and the procedures were shown as following.

2.12.1. Blank detection

The CL intensity of I_0 was measured when only PBS existed in sample tube. I_0 was produced by the pure luminol-H_2O_2 and very low.

2.12.2. Sample detection

LZM and DNAzyme/L-Apt/GQDs@GO@CF existed in sample tube. LZM could specific combine with L-Apt, making DNAzyme release from the composites' surface. Released DNAzyme could catalyze the CL reaction of luminol-H_2O_2 and the CL intensity of I_1 varied strong. So $\Delta I = I_1 - I_0$ was produced by DNAzyme in sample and indirect detection of LZM was realized.

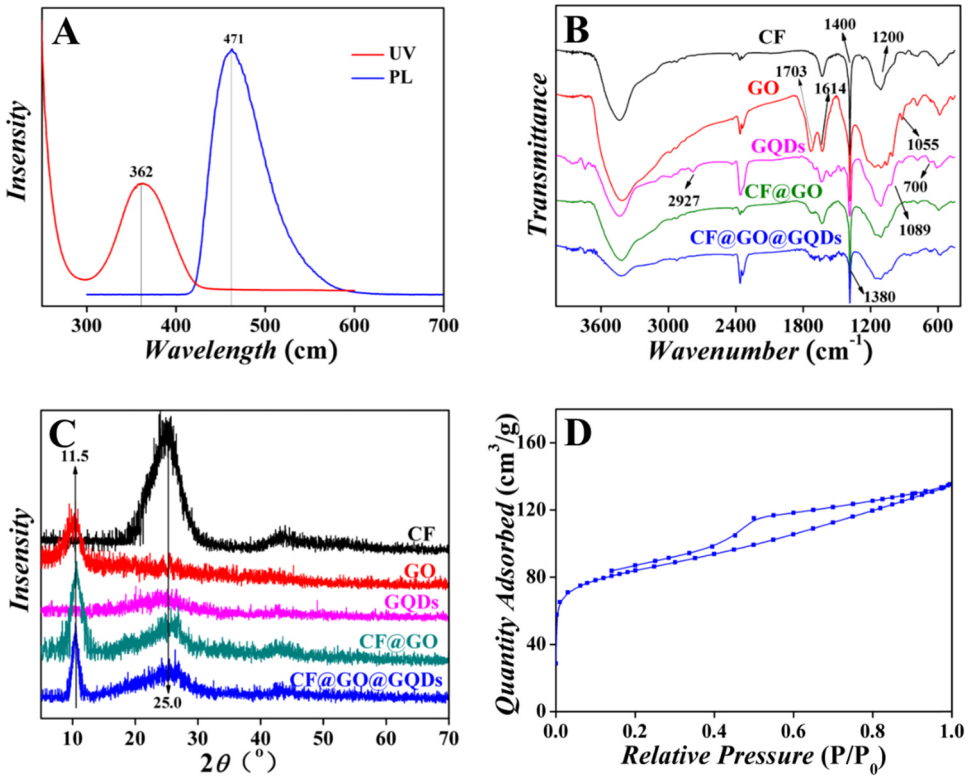

Fig. 4. The UV and FL characterization of GQDs (A); the FTIR (B) and XRD (C) of CF, GO, GQDs, GO@CF and GQDs@GO@CF; the BET characterization curve of GQDs@GO@CF (D).

3. Results and discussion

3.1. Characterizations

As shown in Fig. 3, the surface morphology of GQDs, GO, CF, GO@CF and GQDs@GO@CF were characterized by TEM or SEM. In Fig. 3(A), GQDs presented a bright dark area in its sheet structure. In Fig. 3(B), a wrinkled and thin film was observed, which demonstrated the large specific surface area of GO. Compared with Fig. 3(C), the surface of CF has been fully washed and oxidized in Fig. 3(D). In Fig. 3(E), the surface of CF was successfully coated with a thin layer of GO. Fig. 3(F) clearly reveals GO@CF was successfully modified by another thin layer of GQDs, which could provide greater specific surface area and rich functional groups.

Subsequently, Fig. 4(A) showed the FL and UV characterizations of GQDs. The FL characteristic absorption peak of GQDs appears at 471 nm under the excitation wavelength of 362 nm while the UV spectra shows a characteristic absorption peak at 362 nm. So GQDs was successfully synthesized.

Then, Fig. 4(B) showed the FTIR characterization curves of CF, GO, GQDs, GO@CF and GQDs@GO@CF under the wavenumber range of 400–4000 cm^{-1}. For CF, the absorption peak of 1400 cm^{-1} is attributed to the coupling vibration of -COOH and the peak of 1200 cm^{-1} is the deformation vibration of O-H. For the curve of GO, the absorption peaks at 1703 cm^{-1} and 1614 cm^{-1} belong to the stretching vibration peaks of C=O and C=C, respectively. 1380 cm^{-1} and 1055 cm^{-1} are the deformation vibration peak of O-H and the stretching vibration peak of C-O, respectively. These results showed GO was successfully synthesized. In the spectrum of GQDs, the absorption peaks at 700 cm^{-1}, 2927 cm^{-1} and 1089 cm^{-1} are attributed to the in-plane bending vibration of -OH, the stretching vibration of -OH and the stretching vibration of C-O-C, respectively, which indicates GQDs was successfully prepared. For GO@CF, it also contains the characteristic absorption peaks of GO and CF, which clarified it was successfully synthesized. Similarly, for the curve of GQDs@GO@CF, it also contains the characteristic absorption peaks of GQDs and GO@CF, demonstrating its successful synthesis.

To provide further illustrations, XRD characterizations of CF, GO, GQDs, GO@CF and GQDs@GO@CF were investigated and shown in Fig. 4(C). Obviously, a wide and strong characteristic absorption peak of CF situates around $2\theta = 25.0°$, the characteristic peak of GO is around $2\theta = 11.5°$ and the wide but weak characteristic absorption peak of GQDs lies around $2\theta = 25.0°$. In the spectrums of GO@CF or GQDs@GO@CF, all corresponding diffraction peaks are observed and these satisfying results further provided remarkable supports for their successful preparation.

The BET characterization curve of GQDs@GO@CF was shown in Fig. 4(D). The specific surface area is 268.67 m^2/g and it could provide a relatively large specific surface area to immobilize L-Apt.

3.2. Immobilization properties

To illustrate the excellent immobilization properties of GQDs@GO@CF to L-Apt, the immobilization properties of GO, GO@CF and GQDs@GO@CF were also examined, respectively. The immobilization capacities of L-Apt at different initial concentrations, i.e. the immobilization isotherms, were shown in Fig. 5(A). The immobilization capacity (Q_e) of L-Apt increased with the concentration of L-Apt ($c_{L\text{-}Apt}$) before reaching the maximum capacity of 1.135×10^{-6} g/g, compared to 4.155×10^{-7} g/g of GO and 7.540×10^{-7} g/g of GO@CF. Fig. 5(B) showed the immobilization kinetics of GQDs@GO@CF (GO, GO@CF) to L-Apt and the maximum immobilization capacity of GQDs@GO@CF was easily reached within 15 min, compared to 25 min of GO and 25 min of GO@CF. These satisfied immobilization properties of GQDs@GO@CF may contribute to the strong π-π stacking effect between GQDs@GO@CF and L-Apt.

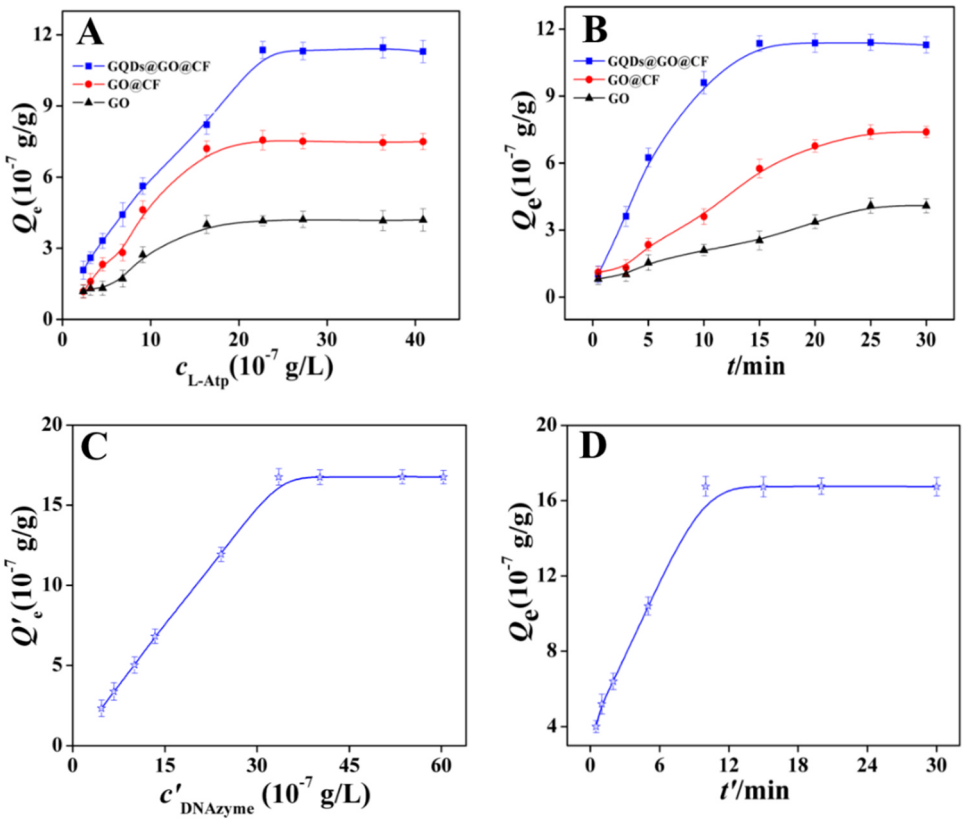

Fig. 5. The immobilization isotherm curves (A) and immobilization kinetics curves (B) of GQDs@GO@CF (GO, GO@CF) to L-Apt; the adsorption isotherm curve (C) and adsorption kinetics curve (D) of L-Apt/GQDs@GO@CF to DNAzyme.

3.3. Adsorption performances

The adsorption performances of L-Apt/GQDs@GO@CF to DNAzyme were also measured. The adsorption capacities of L-Apt/GQDs@GO@CF to DNAzyme at different initial concentrations, i.e. the adsorption isotherms, were shown in Fig. 5(C). The adsorption capacity (Q'_e) for DNAzyme increased with the concentration of DNAzyme ($c'_{DNAzyme}$) before reaching a maximum of 1.676×10^{-6} g/g. Fig. 5(D) showed the adsorption kinetics of L-Apt/GQDs@GO@CF to DNAzyme and the maximum adsorption capacity was easily reached within 10 min, which could be contributed to the electrostatic interaction and fast mass transfer between L-Apt/GQDs@GO@CF and DNAzyme.

3.4. Optimizations

The peristaltic pumps speed was an important parameter for the adsorption amount of DNAzyme on the surface of L-Apt/GQDs@GO@CF. When the speed was too high, DNAzyme could not be absorbed effectively. But when it was too low, other substances could be absorbed by L-Apt/GQDs@GO@CF and interfere LZM detection. Thus, 35 rpm of main pump speed and 30 rpm of vice pump speed were optimized range from 20 to 50 rpm, as showed in Fig. 6(A, B). In addition, the concentrations of luminol, H_2O_2 and NaOH would also affect the CL intensity and were optimized as showed in Fig. 6(C–E). It could be seen that the maximum CL intensity could be obtained at 7.5×10^{-4} mol/L luminol, 0.10 mol/L H_2O_2 and 0.10 mol/L NaOH, simultaneously.

3.5. Analytical performances

Under the optimized conditions, analytical performances of the CL biosensor were studied. In Fig. 6(F), the CL intensity (ΔI) and the concentration of LZM (c_{LZM}) showed a good linear correlation and the calibration curve was $\Delta I = (0.784 \pm 0.00041)\ c_{LZM} + (119.58 \pm 0.028)$, ($c_{LZM}$: 10^{10} mol/L, $\alpha = 0.05$, $R = 0.996$). The detection range was from 2.64×10^{-10} to 6.60×10^{-8} g/L and the detection limit was 1.25×10^{-11} g/L (3δ). Simultaneously, LZM samples with same concentration (5.0×10^{-9} g/L) were measured and the relative standard deviation (RSD) was obtained of 1.79% ($n = 11$). The proposed CL biosensor was also compared with other already existed methods and these results were shown in Table 1. These results indicated the proposed CL biosensor had a relatively wide linear range and low detection limit to LZM detection.

3.6. Selectivity performances

Anti-interference ability of the proposed CL biosensor were also researched. In experiments, different interference substances with high concentrations related to LZM (c_{LZM}: 8.0×10^{-8} g/L) were added in standard LZM solution, respectively. Interference substances contained BSA, Hb, Gly, Cys, ALT, AC, LA, K^+ and Cl^-. The anti-interference ability was also compared with the conventional CL method, shown in Fig. 7(A). The experimental conditions for the conventional CL biosensor were exactly same as the proposed CL biosensor excepting not adding DNAzyme/L-Apt/GQDs@GO@CF. These results showed the interference multiples of proposed CL biosensor had significant increases compared to the conventional CL method. For the proposed CL biosensor, 300 multiples of Cys would interfere the determination of LZM while 70 multiples of conventional CL biosensor. These similar conclusions were also applied to Gly, AC and LA. But for the protein analytes - BSA, Hb and ALT, the increases was not significant, which may attribute to their similar structural units with LZM. For inorganic ions, the prepared CL biosensor exhibited obviously anti-jamming capability, which may due to the weak structural similarity. Therefore, the proposed CL biosensor demonstrated a strong anti-interference ability to LZM detection.

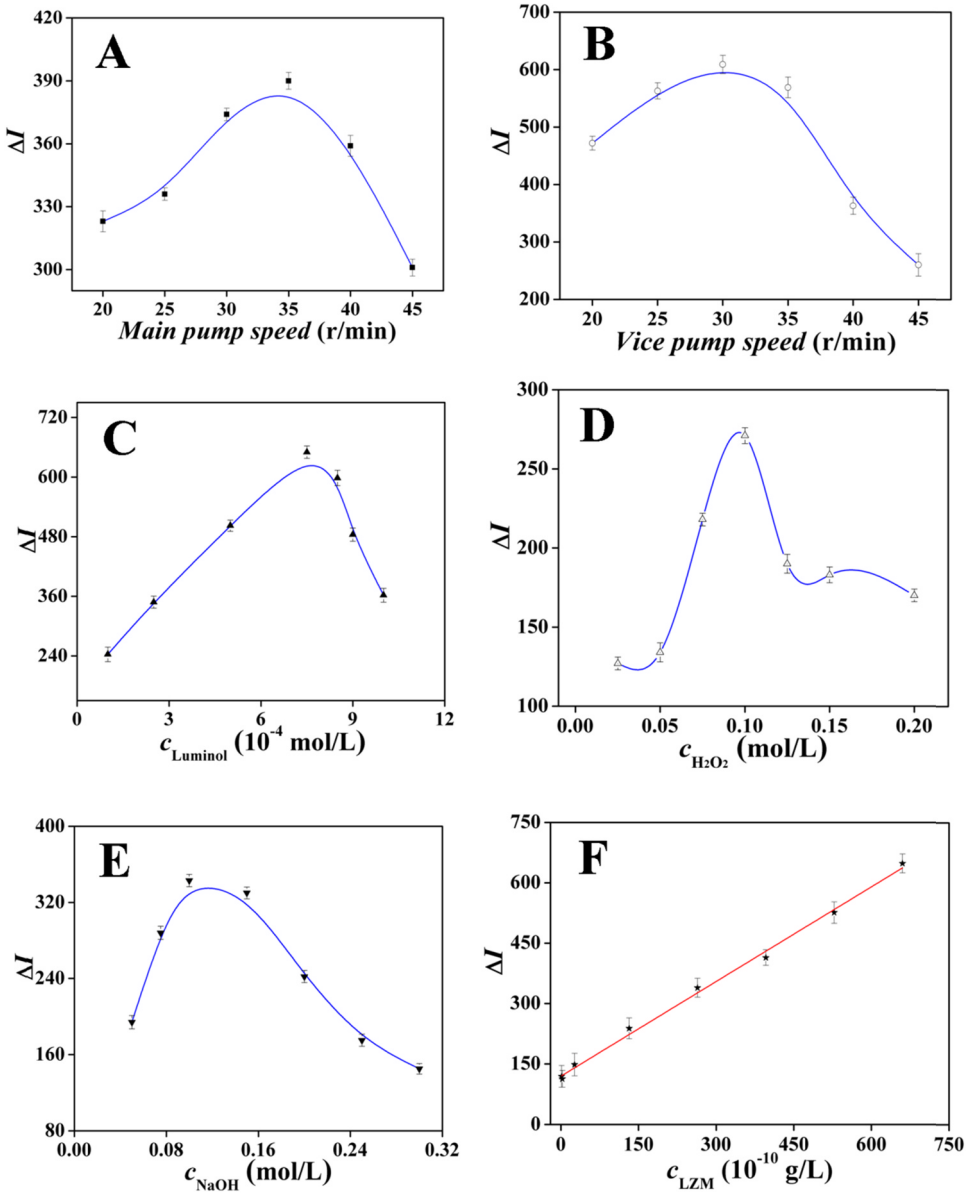

Fig. 6. The CL intensity effects of main pump speed (A), 20 r/min vice pump, 2.5 × 10^{-4} mol/L luminol, 0.10 mol/L H_2O_2 and 0.10 mol/L NaOH; vice pump speed (B), 35 r/min main pump, 30 r/min vice pump, 2.5 × 10^{-4} mol/L luminol, 0.10 mol/L H_2O_2 and 0.10 mol/L NaOH; Luminol (C), 35 r/min main pump, 30 r/min vice pump, 0.10 mol/L H_2O_2 and 0.10 mol/L NaOH; H_2O_2 (D), 35 r/min main pump, 30 r/min vice pump, 7.5 × 10^{-4} mol/L luminol and 0.10 mol/L NaOH; NaOH (E) 35 r/min main pump, 30 r/min vice pump, 7.5 × 10^{-4} mol/L luminol and 0.10 mol/L H_2O_2; the regression equation (F) of the proposed CL biosensor.

3.7. Recyclability performances

The repeatability of prepared composite is an important parameter to evaluate the CL biosensors' practicality. For the proposed CL biosensor, GQDs@GO@CF could be recycled for reuse when a test was completed. When LZM existed, LZM@L-Apt/GQDs@GO@CF was formed. But when conditions change, such as high temperature (95 °C) or highly acidic (pH = 2), LZM@L-Apt would be desorbed from the surface of GQDs@GO@CF and GQDs@GO@CF could be reused. As shown in Fig. 7(B), compared with the original adsorption capacity of 1.135 × 10^{-6} g/g, the adsorption capacity of GQDs@GO@CF to L-Apt used 6 times was 1.086 × 10^{-6} g/g and the adsorption capacity loss was only 4.3%. It manifested that GQDs@GO@CF was suitable to be reused in the construction of CL biosensor.

Table 1
Comparing results with some existed methods.

Analytical method	Linear range (g/L)	Detection limit (g/L)
Proposed	2.64 × 10^{-10}–6.60 × 10^{-8}	1.25 × 10^{-11}
Resonance Rayleigh-scattering [9]	8.0 × 10^{-5}–2.0 × 10^{-3}	6.5 × 10^{-7}
Electrochemical biosensor [10]	5.0 × 10^{-8}–1.0 × 10^{-4}	1.5 × 10^{-8}
Fluorescence [12]	5.0 × 10^{-5}–1.0 × 10^{-3}	3.343 × 10^{-5}
CL method based MIPs polymers [13]	1.0 × 10^{-9}–8.0 × 10^{-8}	3.0 × 10^{-10}
Aptamer-based biosensor [14]	1.0 × 10^{-5}–2.0 × 10^{-3}	1.0 × 10^{-6}

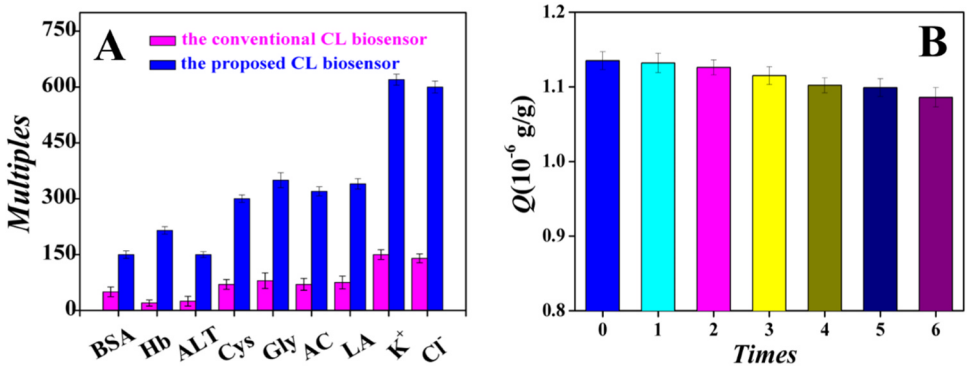

Fig. 7. The selectivity performance (A) and recyclability (B) of the proposed CL biosensor.

Table 2
Application of the proposed CL biosensor.

Sample	c (10^{-9} g/L) (n = 6)	c_{added} (10^{-10} g/L)	c_{found} (10^{-9} g/L) (n = 6)	RSD (%)	Recovery (%)
1	1.21	5.00	11.40	1.71	100.6
2	1.18	5.00	11.51	1.68	99.4
3	1.25	5.00	11.47	1.74	97.5
4	1.19	5.00	11.54	1.68	98.3
5	1.20	5.00	11.52	1.72	103.2
6	1.17	5.00	11.46	1.67	99.9

Male urine samples: 1, 2, 3; female urine samples: 4, 5, 6.

3.8. Application performances

Under the optimal experimental conditions, the proposed CL biosensor was applied in LZM detection in urine samples. The human urine samples were collected from six healthy individuals (3 male and 3 female) and were diluted 10^6-fold with PBS, respectively. The concentrations of LZM in urine samples were calculated as (1.20 ± 0.05) × 10^{-3} g/L by a standard addition method and there was no significant difference between male and female urine samples, which were comparable to the literature values [50]. To calculate the recoveries, urine samples were then spiked with 5.0 × 10^{-10} g/L of LZM, respectively. As shown in Table 2, the proposed method shows excellent recoveries in the range 97.5–103.2%. Therefore, the proposed CL biosensor may provide an alternative method to detect LZM in serum samples or other simple samples.

To further support the proposed CL method for LZM detection, validation experiments were carried out, shown in Table 3. Under optimized experimental conditions, the proposed method and other reported detection methods [13] were all applied to determinate LZM in the same standard samples, respectively. Obviously, the recoveries of the proposed method varied from 98.0% to 100.2% compared with the recoveries of the reported method from 99.8% to 102.0%. These results showed that the proposed method had relatively good precision and accuracy for LZM detection compared with existed method.

3.9. Construction principles and possible mechanisms

In construction of the CL biosensor, GQDs@GO@CF was regarded as a supporting material and provided large binding sites to L-Apt. L-Apt was a specific recognition element and improved the selectivity of the CL biosensor. Moreover, DNAzyme was regarded as a signal amplification material and catalyzed the CL reaction of luminal-H_2O_2, further improving the sensitivity of the CL biosensor. As showed in Fig. 2, primitively, L-Apt was immobilized on the surface of GQDs@GO@CF to form L-Apt/GQDs@GO@CF by the π-π stacking effect. Then, DNAzyme could be adsorbed on the surface of the L-Apt/GQDs@GO@CF by the base complementary pairing effect. When LZM existed, LZM and L-Apt would be specifically bound together, making DNAzyme release from the surface of L-Apt/GQDs@GO@CF. Ultimately, LZM@L-Apt/GQDs@GO@CF was separated and DNAzyme was remained in solution. DNAzyme in solution would catalyze the CL reaction of luminol - H_2O_2 and realized the indirect detection of LZM.

In the CL system of luminal - H_2O_2, H_2O_2, as an oxidizer, could oxidize luminol luminescence in alkaline environment. But the pure reaction is relatively weak. As mentioned in Introduction, DNAzyme as a catalyst can catalyze some CL reaction. For the proposed CL biosensor, possible mechanisms of DNAzyme catalyzing luminal - H_2O_2 was shown in Fig. 8. Hemin has an axial high-spin ferric heme and DNAzyme was formed when hemin bounds to G-quadruplex DNA. Conjuncted with the active sites of G-quadruplex DNA, the coordination of guanine to heme iron could contribute to their superior peroxidase activity. Then, intermediates DNAzyme-H_2O_2 is generated in the presence of H_2O_2. Under alkaline environment, luminol is oxidized by DNAzyme-H_2O_2 to generate luminol-acid radical ion and produces the stronger CL indensity. These possible CL mechanisms are consistent with the literatures [51–53].

4. Conclusions

Highly sensitive, selective and accurate detection of LZM is of particular significant owing to its important role in food preservation, biochemical research and disease treatment fields. For the proposed CL

Table 3
Validation experiments of the detection method ($\bar{x}$ ± s).

Sample	c (10^{-9} g/L) (n = 6)	c_{added} (10^{-9} g/L)	c_{found} (10^{-9} g/L) (n = 6)	RSD (%)	Recovery (%)
1	5.01 ± 0.032*	1.00	5.99 ± 0.013*	1.8 ± 0.011	98.0 ± 0.12
1′	4.98 ± 0.023	1.00	6.00 ± 0.012	2.3 ± 0.013	102.0 ± 0.14
2	5.00 ± 0.028*	3.00	7.98 ± 0.021*	2.4 ± 0.011	99.3 ± 0.082
2′	5.00 ± 0.012	3.00	8.01 ± 0.016	1.6 ± 0.0094	100.3 ± 0.22
3	4.97 ± 0.015*	5.00	9.98 ± 0.019*	2.2 ± 0.012	100.2 ± 0.19
3′	5.01 ± 0.026	5.00	9.99 ± 0.0074	2.6 ± 0.078	99.8 ± 0.098

The proposed method: sample 1, 2, 3; the reported method: sample 1′, 2′, 3′.
* $P < 0.05$ *vs* the reported method.

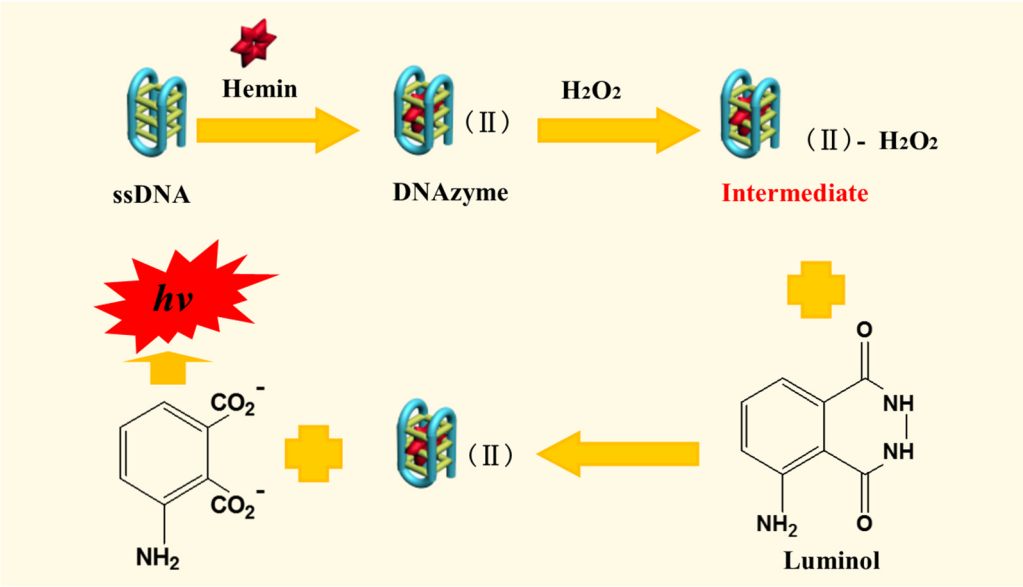

Fig. 8. The possible chemiluminescence mechanism of the CL biosensor.

biosensor, the sandwich-rod composite - DNAzyme/L-Apt/GQDs@GO@CF was successfully prepared and used to the construction of CL biosensor for LZM detection. GQDs@GO@CF had good biocompatibility and provided large binding sites to L-Apt. As a specific recognition element, L-Apt improved the biosensors' selectivity owing to the specific recognition ability between L-Apt and LZM. DNAzyme catalyzed the CL reaction of luminal-H_2O_2 and further improved the biosensors' sensitivity. So the proposed CL biosensor for LZM detection showed highly sensitivity with detection limit of 1.25×10^{-11} g/L, wide linear range of 2.64×10^{-10} to 6.60×10^{-8} g/L and recoveries in the range of 97.5–103.2% in urine samples. So the proposed CL biosensor provides a potential application value for LZM detection in pratical samples.

Acknowledgements

This work was supported by National Science Foundation for Young Scientists of China (No. 21605094), Shandong Province Natural Science Institute Joint Fund (No. ZR2015YL006), Natural Science Foundation of Shandong Province, China (No. ZR2016BM01) and Horizontal Scientific Research Project of China (No. W15077).

References

[1] R. Zhang, L. Wu, T. Eckert, M. Burg-Roderfeld, M.A. Rojas-Macias, et al., Lysozyme's lectin-like characteristics facilitates its immune defense function, Q. Rev. Biophys. 50 (2017) 1–12.
[2] L. Wang, L. Li, Y. Xu, G. Cheng, P. He, et al., Simultaneously fluorescence detecting thrombin and lysozyme based on magnetic nanoparticle condensation, Talanta 79 (3) (2009) 557–561.
[3] V.A. Proctor, F.E. Cunningham, The chemistry of lysozyme and its use as a food preservative and a pharmaceutical, Crit. Rev. Food Sci. Nutr. 26 (4) (1988) 359–395.
[4] B.G. Libman, K.A. Kagramanova, Z.V. Ermol'Eva, Use of lysozyme in medicine, Sov. Med. 34 (11) (1971) 34–40.
[5] A.A. Pokrovskii, V.A. Tutel'ian, Current concepts of lysosomes, Uspekhi Sovrem. Biol. 68 (3) (1969) 318–339.
[6] B. Pawel, K. Mehta, A case of acute monocytic leukemia with lysozyme-positive leukemic monocytes and normal serum lysozyme levels, Acta Haematol. 81 (1989) 101–103.
[7] C. Sexton, D. Buss, B. Powell, M. O'Connor, R. Rainer, et al., Usefulness and limitations of serum and urine lysozyme levels in the classification of acute myeloid leukemia: an analysis of 208 cases, Leuk. Res. 20 (6) (1996) 467–472.
[8] Y. Xie, J. An, P. Shi, N. Ye, Determination of lysozyme by graphene oxide-polyethylene glycol-based fluorescence resonance energy transfer, Anal. Lett. 50 (1) (2017) 148–160.
[9] Z. Cai, G. Chen, X. Huang, M. Ma, Determination of lysozyme at the nanogram level in chicken egg white using Resonance Rayleigh-scattering method with Cd-doped ZnSe quantum dots as probe, Sens. Actuators B: Chem. 157 (2011) 368–373.
[10] Z. Zhang, S. Zhang, L. He, D. Peng, F. Yan, et al., Feasible electrochemical biosensor based on plasma polymerizationassisted composite of polyacrylic acid and hollow TiO_2 spheres for sensitively detecting lysozyme, Biosens. Bioelectron. 74 (2015) 384–390.
[11] F. Ahour, M.K. Ahsani, An electrochemical label-free and sensitive thrombin aptasensor based on graphene oxide modified pencil graphite electrode, Biosens. Bioelectron. 86 (2016) 764–769.
[12] X. Fu, X. Fu, Q. Wang, L. Sheng, X. Huang, et al., Fluorescence switch biosensor based on quantum dots and gold nanoparticles for discriminative detection of lysozyme, Int. J. Biol. Macromol. 103 (2017) 1155–1161.
[13] H. Duan, X. Wang, Y. Wang, Y. Sun, J. Li, et al., An ultrasensitive lysozyme chemiluminescence biosensor based on surface molecular imprinting using ionic liquid modified magnetic graphene oxide/β-cyclodextrin as supporting material, Anal. Chim. Acta 918 (2016) 89–96.
[14] J. Wu, Y. Hou, P. Wang, Z. Wang, Y. Li, et al., Detection of lysozyme with aptasensor based on fluorescence resonance energy transfer from carbon dots to graphene oxide, Luminescence 31 (6) (2016) 1207–1212.
[15] T. Lou, H. Qiang, Z. Chen, Core-shell Cu@Au nanoparticles-based colorimetric aptasensor for the determination of lysozyme, Talanta 163 (2017) 132–139.
[16] N. Siraj, B. El-Zahab, S. Hamdan, T.E. Karam, L.H. Haber, et al., Fluorescence, phosphorescence, and chemiluminescence, Anal. Chem. 88 (1) (2016) 170–202.
[17] G. Chen, M. Jin, P. Du, C. Zhang, X. Cui, et al., A sensitive chemiluminescence enzyme immunoassay based on molecularly imprinted polymers solid-phase extraction of parathion, Anal. Biochem. 530 (2017) 87–93.
[18] G. Chen, M. Jin, P. Du, C. Zhang, X. Cui, et al., A review of enhancers for chemiluminescence enzyme immunoassay, Food Agric. Immunol. 28 (2) (2017) 315–327.
[19] S. Li, X. Wu, C. Liu, G. Yin, J. Luo, et al., Application of DNA aptamers as sensing layers for detection of carbofuran by electrogenerated chemiluminescence energy transfer, Anal. Chim. Acta 941 (2016) 94–100.
[20] Y. Sun, X. Wang, H. Xu, C. Ding, Y. Lin, et al., A chemiluminescence aptasensor for thrombin detection based on aptamer-conjugated and hemin/G-quadruplex DNAzyme signal-amplified carbon fiber composite, Anal. Chim. Acta 1043 (2018) 132–141.
[21] Y. Su, Y. Xie, X. Hou, Y. Lv, Recent advances in analytical applications of nanomaterials in liquid-phase chemiluminescence, Appl. Spectrosc. Rev. 49 (2014) 201–232.
[22] S. Han, Z. Zhang, S. Li, Li Qi, G. Xu, Chemiluminescence and electrochemiluminescence applications of metal nanoclusters, Sci. China Chem. 59 (7) (2016) 794–801.
[23] H. Chen, Q. Gao, J. Li, J. Lin, Graphene materials-based chemiluminescence for sensing, J. Photochem. Photobiol. C: Photochem. Rev. 27 (2016) 54–71.
[24] P. Zou, Y. Liu, H. Wang, J. Wu, F. Zhu, et al., G-quadruplex DNAzyme-based chemiluminescence biosensing platform based on dual signal amplification for label-free and sensitive detection of protein, Biosens. Bioelectron. 79 (2016) 29–33.
[25] Y. He, J. Sun, X. Wang, L. Wang, Detection of human leptin in serum using chemiluminescence immunosensor: signal amplification by hemin/G-quadruplex DNAzymes and protein carriers by Fe_3O_4/polydopamine/Au Nanocomposites, Sens. Actuators B 221 (2015) 792–798.
[26] S. Ni, H. Yao, L. Wang, J. Lu, F. Jiang, et al., Chemical modifications of nucleic acid aptamers for therapeutic purposes, Int. J. Mol. Sci. 18 (8) (2017) 1683.
[27] Y. Yang, S. Yin, Y. Li, D. Lu, J. Zhang, et al., Application of aptamers in detection and chromatographic purification of antibiotics in different matrices, TrAC Trends

Anal. Chem. 95 (2017) 1–22.
[28] L. Farzina, M. Shamsipur, S. Sheibani, A review: aptamer-based analytical strategies using the nanomaterials for environmental and human monitoring of toxic heavy metals, Talanta 174 (2017) 619–627.
[29] Z. Si, B. Xie, Z. Chen, C. Tang, T. Li, et al., Electrochemical aptasensor for the cancer biomarker CEA based on aptamer induced current due to formation of molybdophosphate, Microchim. Acta 184 (9) (2017) 3215–3221.
[30] Z. Zhang, C. Guo, S. Zhang, L. He, M. Wang, et al., Carbon-based nanocomposites with aptamer-templated silver nanoclusters for the highly sensitive and selective detection of platelet-derived growth factor, Biosens. Bioelectron. 89 (2017) 735–742.
[31] W. Lu, M. Zu, J. Byun, B. Kim, T. Chou, State of the art of carbon nanotube fibers: opportunities and challenges, Adv. Mater. 24 (14) (2012) 1805–1833.
[32] E. Frank, L. Steudle, D. Ingildeev, J.M. Spörl, M.R. Buchmeiser, et al., Carbon fibers: precursor systems, processing, structure, and properties, Angew. Chem. Int. Ed. 53 (2014) 5262–5298.
[33] D.D.L. Chung, Processing-structure-property relationships of continuous carbon fiber polymer-matrix composites, Mater. Sci. Eng.: R: Rep. 113 (2017) 1–29.
[34] L. Liu, C. Jia, J. He, F. Zhao, D. Fan, Interfacial characterization, control and modification of carbon fiber reinforced polymer composites, Compos. Sci. Technol. 121 (2015) 56–72.
[35] X. Cai, C. Zhang, S. Zhang, Y. Fang, D. Zou, Application of carbon fibers to flexible, miniaturized wire/fiber-shaped energy conversion and storage devices, J. Mater. Chem. A 5 (2017) 2444–2459.
[36] X. Mao, W. Tian, T.A. Hatton, G.C. Rutledge, Advances in electrospun carbon fiber-based electrochemical sensing platforms for bioanalytical applications, Anal. Bioanal. Chem. 408 (5) (2016) 1307–1326.
[37] G. Shi, Y. Zhang, B. Chen, G. Wang, A novel strategy for the determination of lappaconitine with use of electrostatic spinning carbon nanotube fiber modified glassy carbon electrode, Int. J. Electrochem. Sci. 12 (2017) 3826–3839.
[38] I.M. Taylor, E.M. Robbins, K.A. Catt, P.A. Cody, C.L. Happe, et al., Enhanced dopamine detection sensitivity by PEDOT/graphene oxide coating on in vivo carbon fiber electrodes, Biosens. Bioelectron. 89 (2017) 400–410.
[39] K.S. Novoselov, A.K. Geim, S.V. Morozov, D. Jiang, Y. Zhang, et al., Electric field effect in atomically thin carbon films, Science 306 (5696) (2004) 666–669.
[40] C. Zhu, D. Du, Y. Lin, Graphene-like 2D nanomaterial-based biointerfaces for biosensing applications, Biosens. Bioelectron. 89 (2017) 43–55.
[41] D.C. Marcano, D.V. Kosynkin, J.M. Berlin, A. Sinitskii, Z. Sun, et al., Improved synthesis of graphene oxide, ACS Nano 4 (8) (2010) 4806–4814.
[42] X. Chen, X. Hai, J. Wang, Graphene/graphene oxide and their derivatives in the separation/isolation and preconcentration of protein species: a review, Anal. Chim. Acta 922 (2016) 1–10.
[43] K. Zhang, Q. Fu, N. Pan, X. Yu, J. Liu, et al., Direct writing of electronic devices on graphene oxide by catalytic scanning probe lithography, Nat. Commun. 3 (6) (2012) 1194–1199.
[44] J. Xu, Y. Wang, S. Hu, Nanocomposites of graphene and graphene oxides: synthesis, molecular functionalization and application in electrochemical sensors and biosensors. A review, Microchim. Acta 184 (1) (2017) 1–44.
[45] F. Li, X. Jiang, J. Zhao, S. Zhang, Graphene oxide: a promising nanomaterial for energy and environmental applications, Chem. Rev. 16 (2015) 488–515.
[46] X. Zhou, S. Guo, J. Zhang, Solution-processable graphene quantum dots, ChemPhysChem Eur. J. Chem. Phys. Phys. Chem. 14 (2013) 2627–2640.
[47] Y. Dua, S. Guo, Chemically doped fluorescent carbon and graphene quantum dots for bioimaging, sensor, catalytic and photoelectronic applications, Nanoscale 8 (2016) 2532–2543.
[48] X. Sun, Z. Liu, H. Yan, Preparation of graphene quantum dots and their biological applications, J. Inorg. Mater. 31 (2016) 337–344.
[49] W.S. Hummers, R.E. Offeman, Preparation of graphitic oxide, J. Am. Chem. Soc. 80 (1958) 1339.
[50] L. Callewaert, C.W. Michiels, Lysozymes in the animal kingdom, J. Biosci. 35 (1) (2010) 127–160.
[51] X. Zhu, W. Zhang, H. Xiao, J. Huang, G. Li, Electrochemical study of a Hemin-DNA complex and its activity as a ligand binder, Electrochim. Acta 53 (2008) 4407–4413.
[52] P. Travascio, Y. Li, D. Sen, DNA-enhanced peroxidase activity of a DNA aptamer-hemin complex, Chem. Biol. 5 (1998) 505–517.
[53] P. Travascio, P.K. Witting, A.G. Mauk, D. Sen, The peroxidase activity of a Hemin-DNA oligonucleotide complex: free radical damage to specific guanine bases of the DNA, J. Am. Chem. Soc. 123 (2001) 1337–1348.